Detection of adulteration in hydrated ethyl alcohol fuel using infrared spectroscopy and supervised pattern recognition methods

Adenilton Camilo Silva[a], Liliana Fátima Bezerra Lira Pontes[a], Maria Fernanda Pimentel[b], Márcio José Coelho Pontes[a],*

[a] Universidade Federal da Paraíba, Departamento de Química, João Pessoa, PB, Brazil
[b] Universidade Federal de Pernambuco, Departamento de Engenharia Química, Recife, PE, Brazil

ARTICLE INFO

ABSTRACT

This paper proposes an analytical method to detect adulteration of hydrated ethyl alcohol fuel based on near infrared (NIR) and middle infrared (MIR) spectroscopies associated with supervised pattern recognition methods. For this purpose, linear discriminant analysis (LDA) was employed to build a classification model on the basis of a reduced subset of wavenumbers. For variable selection, three techniques are considered, namely the successive projection algorithm (SPA), the genetic algorithm (GA) and a stepwise formulation (SW). For comparison, models based on partial least squares discriminant analysis (PLS-DA) were also employed using full-spectrum. The method was validated in a case study involving the classification of 181 hydrated ethyl alcohol fuel samples, which were divided into three different classes: (1) authentic samples; (2) samples adulterated with water and (3) samples contaminated with methanol. LDA/GA and PLS-DA models were found to be the best methods for classifying the spectral data obtained in NIR region, which achieved a correct prediction rate of 100% in the test set, while the LDA/SPA and LDA/SW were correctly classified at 84.4% and 97.8%, respectively. For MIR data, all models (PLS-DA and LDA coupled with the SW, SPA and GA) employed in this study correctly classified all samples in the test set.

© 2012 Elsevier B.V. All rights reserved.

1. Introduction

Ethanol is frequently used as raw material for beverages, cosmetics, pharmaceuticals and in the chemical industries. Due to the variety of renewable resources available in Brazil, ethanol is widely used as an automotive vehicle fuel [1,2]. This is usually found in an anhydrous form (blended with the gasoline) and as hydrated ethyl alcohol fuel (HEAF) [3].

According to the Brazilian National Agency for Petroleum, Natural Gas, and Biofuels (ANP) the HEAF has had, in recent years, one of the highest rates of nonconformity among all fuels monitored in Brazil [4]. The main form of adulteration in HEAF samples is the illegal addition of water to ethanol fuel or, in more serious cases, replacement of ethyl alcohol by methyl alcohol. According to Resolution ANP [5], the permitted maximum levels of water and methanol in HEAF samples are 4.9% ($v\,v^{-1}$) and 1.0% ($v\,v^{-1}$), respectively.

Methanol and ethanol present similar physical–chemical properties, including: solubility in water, density values, look and smell [6]. The lower price of methanol in relation to ethanol and the similarity of these alcohols contribute to the ease of adulteration of HEAF with methanol in Brazil. Methanol is extremely toxic and can cause serious health problems such as headache, nausea, vomiting, blindness and even death. Therefore it is against the law for it to be used as fuel in Brazil [7].

The reference method to measure alcohol content in HEAF samples is based on the ABNT NBR 5992 standard [8]. This method uses a glass hydrometer to measure the alcohol content; but it is not possible to distinguish the type of alcohol (ethyl or methyl) in the HEAF samples. The Brazilian Standards Association (ABNT) has elaborated a draft standard (draft 34:007.01-006), now in the public enquiry stage, to determine the amount of ethanol and methanol concentration in ethanol fuel samples with a method based on gas chromatography.

Considering the possibility of HEAF adulteration with water or methanol, it is important to develop a fast, simple and low cost method able to detect whether the permitted maximum levels of

* Corresponding author at: Universidade Federal da Paraíba, Departamento de Química – Laboratório de Automação e Instrumentação em Química Analítica/Quimiometria (LAQA), CEP 58051-970, João Pessoa, PB, Brazil. Tel.: +55 83 3216 7438; fax: +55 83 3216 7438.
E-mail addresses: marcio.quimica@gmail.com, marciocoelho@quimica.ufpb.br (M.J.C. Pontes).

these solvents in HEAF samples fall within those allowed by Brazilian legislation.

Infrared spectroscopy (IR) is an alternative non-destructive analytical technique which allows reliable, direct and fast determination of several properties at the same time without sample pre-treatment [2,9,10]. Several papers have been reported in the literature exploring the use of near infrared (NIR) and middle infrared (MIR) spectroscopies associated with multivariate analysis to monitor the quality of fuel and biofuels [2,9–16].

Felizardo et al. [11] used NIR spectroscopy to determine the content of water and methanol in biodiesel. For this, models based on partial least square (PLS) and principal component regression (PCR) were employed. Fernandes et al. [12] used NIR spectroscopy with PLS models for the simultaneous determination of methanol and ethanol contents in gasoline. Fourier transform-near infrared (FT-NIR) and FT-Raman spectrometries have been used to determine the content of ethanol in ethanol fuel [13].

With respect to hydrated ethyl alcohol fuel, only one paper [14] has been published using IR spectroscopy to detect the adulteration of HEAF with water and methanol. The authors used a quantitative multivariate method based on PLS to determine the content of ethanol, water and methanol in HEAF samples. Explicit studies regarding the detection of adulteration in these samples by using infrared spectroscopy associated to supervised pattern recognition methods have not been found in the specialized literature.

Pattern recognition methods [17] such as partial least squares discriminant analysis (PLS-DA) [18] and linear discriminant analysis (LDA) [19] have been applied extensively in classification problems [20–23]. PLS-DA is based on the standard PLS algorithm, using class labels as dependent **y** vector. The PLS2 algorithm is generally employed when the application involves more than two classes. The theoretical basis for PLS-DA can be found in Ref. [18].

The LDA classification method employs linear decision boundaries, which are defined in order to maximize the ratio of between-class to within-class dispersion [19]. In this method, the number of training samples must be larger than the number of variables to be included in the LDA model. Therefore, procedures based on selection of each variable are required for the classification of spectral data. The successive projections algorithm (SPA) [24–30] has been adopted for this purpose in different classification problems, including the analysis of edible vegetable oils [26,31], diesel oils [26], Brazilian soils [32], cigarettes [33], coffee [34] and diesel/biodiesel [35] samples.

In the present paper, an analytical method to detect the adulteration of hydrated ethyl alcohol fuel with methanol and water using NIR and MIR spectroscopies is proposed. For this, LDA is employed to build a classification model on the basis of a reduced subset of spectral variables, selected using three different techniques: successive projection algorithm (SPA) [26], the genetic algorithm (GA) [26,32], and a stepwise formulation (SW) [36]. For comparison purposes, models based on PLS-DA are have also been employed using full-spectrum. The results obtained from these four methods (LDA/SPA, LDA/GA, LDA/SW and PLS-DA) have been assessed in terms of classification errors in a set of samples not used in the model-building process (test samples).

2. Materials and methods

2.1. Samples

One hundred and eighty-one samples of three different classes were analyzed: authentic HEAF samples (60); HEAF samples adulterated with water (61) and HEAF samples contaminated with methanol (60). Adulteration levels with methanol and water were $1–18\%\,m\,m^{-1}$ and $0.5–10\%\,m\,m^{-1}$, respectively. In order to include variety in the adulterated sample composition, the blends were prepared from different samples of HEAF.

2.2. NIR and MIR spectra measurements

A FTLA 2000-160 FTIR spectrophotometer (Bomem) equipped with a quartz cell with an optical path of 1.0 mm was employed to obtain NIR spectra in the range of 7449–3769 cm^{-1} (1342–2653 nm) and a Varian 640 FTIR spectrophotometer equipped with an ATR sampling accessory was used to obtain the FT-IR spectra in the MIR range of 3477–698 cm^{-1} (2876–14327 nm).

All spectra were recorded with an average of 32 scans, and a spectral resolution of 8 cm^{-1}. The background spectra were obtained using a clean empty cell or the ATR accessory. Temperature was controlled at $23 \pm 1\,°C$ throughout the spectral acquisition process.

2.3. Data analysis and software

Raw and derivative (Savitzky–Golay [37], varying the number of window points of 7, 11, 15 and 21) spectra were evaluated for the classification models. Detection and elimination of outliers were carried out using score, residual and leverage plots. The data sets were divided into training, validation and test subsets by using the classic Kennard–Stone (KS) algorithm [38] The KS algorithm was applied to each class separately, as described by Pontes et al. [26]. The number of samples in each data set is presented in Table 1. All spectral data were mean-centered before modeling procedures.

The present work adopts the SPA formulation presented by Pontes et al. [26], in which the validation samples are used in order to choose the best subset of wavenumbers by minimising the cost function (Eq. (1)), defined as an average risk of misclassification by LDA.

$$G = \frac{1}{Kv} \sum_{k=1}^{Kv} g_k, \tag{1}$$

where g_k is the risk of misclassification of the kth validation object $\mathbf{x}_k$, $k = 1,\ldots,Kv$).

The stepwise (SW) selection algorithm utilized in this work calculates the discriminability of each variable (wavenumber) in relation to the classes under consideration [36]. The wavenumber with the largest discriminability value is selected and a leave-one-out cross-validation procedure is carried out by using LDA. In order to avoid collinearity problems, the remaining wavenumbers which present a large correlation with the selected one are discarded. This process is repeated at each subsequent iteration by successively adding wavenumbers to the LDA model until no more wavenumbers are available for selection. The subset of variables leading to the smallest number of cross-validation errors is then adopted. In this algorithm, a threshold value for the coefficient of multiple correlation needs to be defined in order to decide which wavenumbers are to be discarded. In this work, seven threshold values (0.10, 0.30, 0.50, 0.70, 0.80, 0.90, and 0.95) of multiple correlation coefficients were tested in the LDA/SW algorithm. The best threshold was selected on the basis of the classification errors in the validation set.

The present work adopts the GA formulation presented by Pontes et al. [26], where a fitness value was defined for each chromosome as the inverse of the validation cost defined in Eq. (1). The GA routine was carried out over 100 generations with 200 chromosomes in each generation. Mutation and crossover probabilities were set to 10% and 60%, respectively, as in [26]. Moreover, the algorithm was repeated ten times, starting from different random initial populations. The best solution (in terms of the fitness value) resulting from the ten realizations of the GA was employed.

Table 1
Number of training, validation and test samples in each class.

Class	NIR data			MIR data		
	Training	Validation	Test	Training	Validation	Test
Authentic samples	30	15	15	28	15	15
Adulterated with water	31	15	15	28	16	16
Adulterated with methanol	30	15	15	28	14	14
Total	91	45	45	84	45	45

In the case of PLS-DA, each object was associated with one of the three following vectors [1,0,0], [0,1,0], and [0,0,1], representing classes 1, 2 and 3, respectively. A value close to zero indicates that the new sample does not belong to the class under consideration and a value close to one indicates that it belongs. In this work, the threshold value adopted for PLS-DA models was 0.5. When a value above the 0.5 is predicted, a sample is considered to belong to the class under study, while a value below the 0.5 indicates that the sample does not.

PLS-DA was carried out using Unscrambler® X.1 (CAMO S.A.). The KS, LDA-SPA, LDA-SW and LDA-GA algorithms were coded in Matlab (Mathworks, USA).

3. Results and discussion

3.1. NIR and MIR spectra

Fig. 1a presents the original mean NIR spectra of the three classes recorded in the range of 7449–3769 cm^{-1}. These NIR spectra show bands assigned to the first overtones (5000–6000 cm^{-1}) and the combination regions 4600–4000 cm^{-1} of C—H stretching [39]. Additionally, at 6870 cm^{-1}, the first OH overtone of water and ethanol occurs. Combination bands of stretching and angular bending of the OH in water occur at 5128 cm^{-1} [40,41].

Fig. 1b shows the original mean MIR spectra of the three classes recorded in the range of 3477–698 cm^{-1}. It is possible to observe peaks around 1180–840 cm^{-1} corresponding to C—O and C—C—O stretching modes [14]. C—H stretching and water band absorption peaks can be observed at 2900 cm^{-1} and 3450 cm^{-1}, respectively.
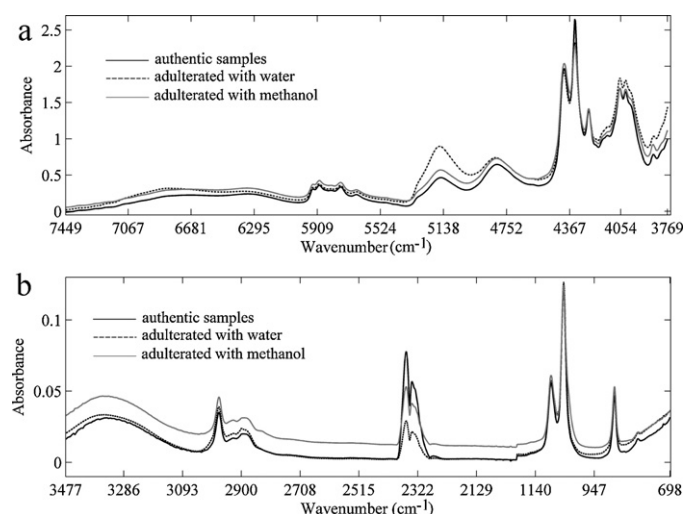
3.2. LDA and PLS-DA classification

The variables selected by SW, SPA and GA for the NIR and MIR data are presented in Fig. 2a–c and Fig. 3a–c, respectively.

It can be observed that the most of the wavenumbers selected by SW and SPA (Fig. 2a and b) are located in the region between 5260 cm^{-1} and 4760 cm^{-1}, which can be attributed to combination bands of O—H bond in the alcohol samples [41]. The SPA algorithm also selected peaks at 4330 cm^{-1} and 4260 cm^{-1}, which may be associated with the second overtone of —CH— bending and with the combination of —CH— stretches, respectively [42]. Peaks around 4000 and 3760 cm^{-1} were selected for SPA and GA algorithms, corresponding to the combination region of C—H vibration. The isolated wavenumber selected by SPA at 7441 cm^{-1} (Fig. 2b) may be associated with the combination region of C—H stretching. The GA algorithm also selected variables around 5867 cm^{-1}, which can be attributed to the (—CH$_2$) methyl group [42].

Fig. 3a–c shows the average MIR spectra of the HEAF samples with variables selected by SW, SPA and GA algorithms. Peaks between 1180 cm^{-1} and 840 cm^{-1} (C—O and C—C—O stretching) [14] were selected by both SW and GA algorithms (Fig. 3a and c). In addition, GA and SW selected several variables around 3000 cm^{-1} and 2900 cm^{-1} corresponding to C—H stretching [42]. Important variables at 3450 cm^{-1} and 698 cm^{-1} were selected by SPA (Fig. 3b), which can be associated to the absorption band of water and asymmetric H—C—H angular deformation of the CH$_2$, respectively.

The LDA models obtained with the variables selected by SW, SPA and GA algorithms were applied to the classification of the test set. Table 2 presents the classification results of LDA/SW, LDA/SPA, LDA/GA and PLS-DA models which were applied to the test set using NIR and MIR data. In both data (NIR and MIR), the best results were achieved with the original spectra (without preprocessing).

The values presented in Table 2 express both correct classifications (predicted class index equal to correct class index) and incorrect classifications (predicted class index different from correct class index). When the NIR spectra was used, the worst overall results of LDA models in terms of classification errors for the test set were obtained with LDA/SW, which correctly classified 38 of the 45 test samples. This outcome corresponds to a correct prediction rate of 84.4%. In contrast, the best results of LDA models were achieved with GA. However, it is worth noting that GA-LDA selected a larger number of spectral variables (17), than SW (2) and SPA (12). In the case of the LDA/SPA model, only one sample belonging to class 2 (HEAF adulterated with water) was classified as belonging to class 1 (authentic HEAF). The classification performance of PLS-DA models was similar to LDA/GA, which correctly classified all samples in the test set.

When the MIR spectra were used, all models (LDA/SW, LDA/SPA, LDA/GA, and PLS-DA) achieved a correct prediction rate of 100% in the test set.

The satisfactory classification performance of LDA models built with variable selected is further demonstrated by Fig. 4a–f, which illustrates the scores of the first two discriminant functions (DF2 × DF1) for the overall data set in the NIR and MIR regions. It is possible to observe that the best discrimination is found in the NIR
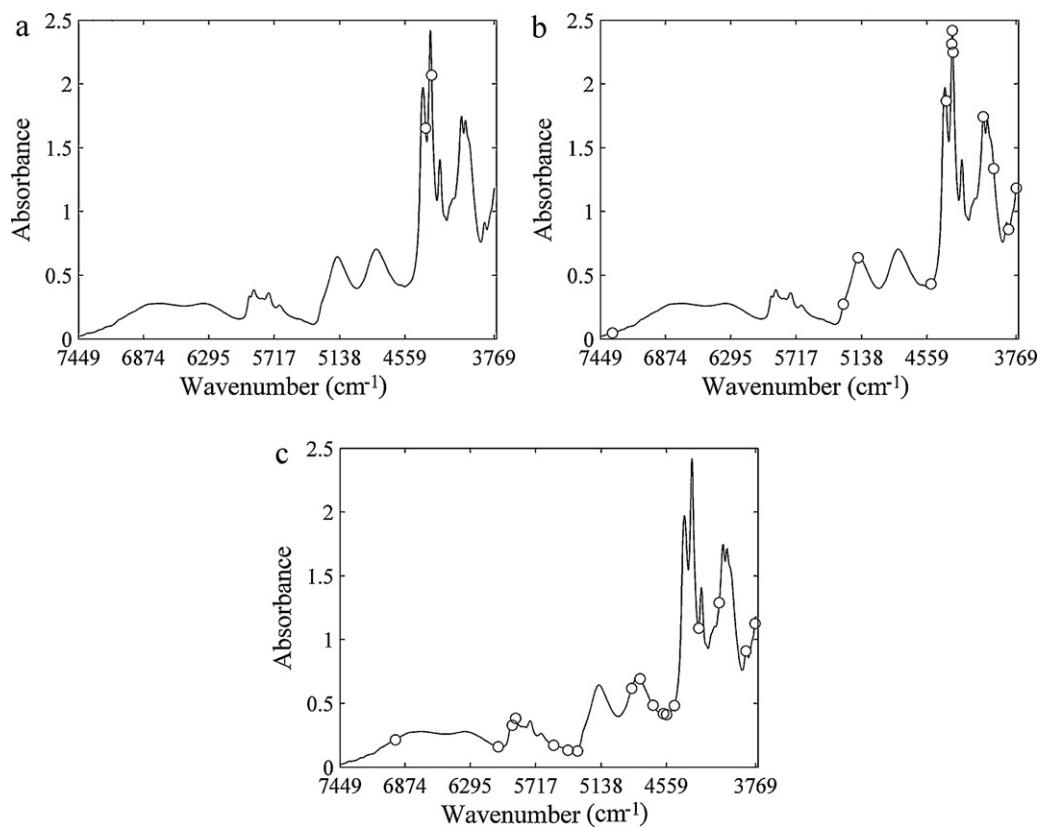

Fig. 1. Original mean spectra of three HEAF samples classes recorded in the region of (a) NIR and (b) MIR.

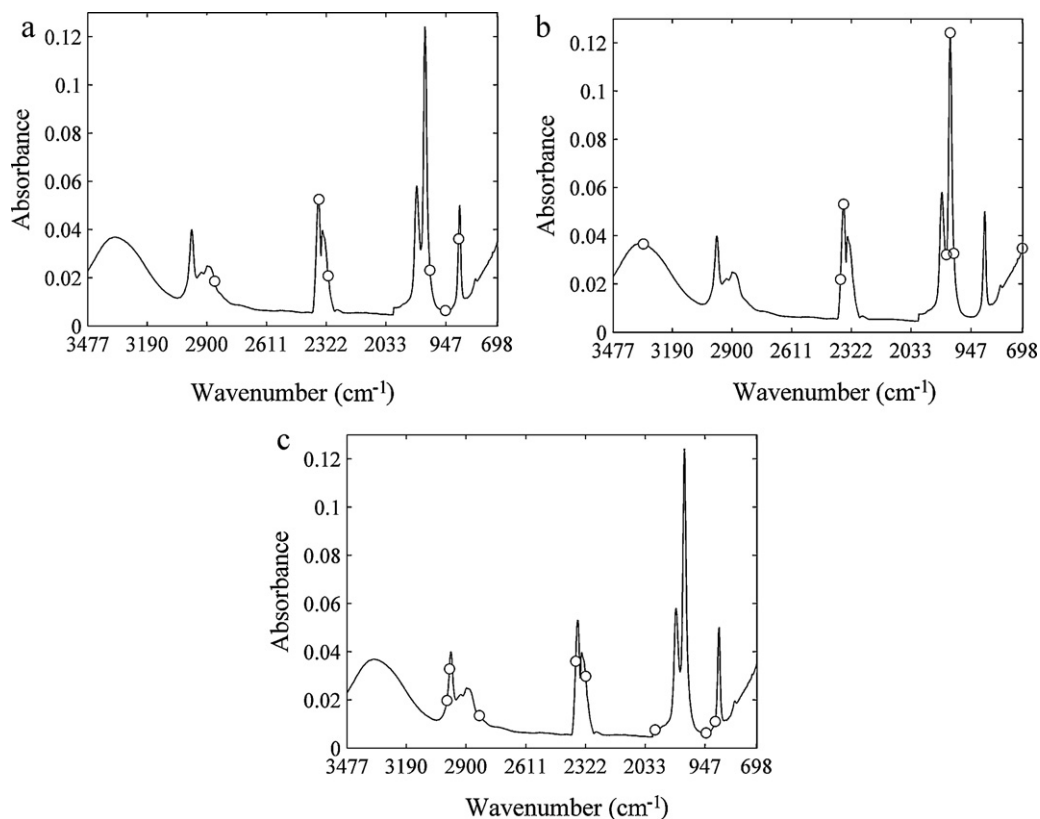**Fig. 2.** Mean NIR spectra with wavenumbers selected by (a) SW, (b) SPA and (c) GA.

Fig. 3. Mean MIR spectra with wavenumbers selected by (a) SW, (b) SPA and (c) GA.

Table 2
Final classification results obtained with LDA/SW, LDA/SPA, LDA/GA and PLS-DA models in the test set. (1) Authentic samples, (2) HEAF adulterated with water and (3) HEAF adulterated with methanol. The number of wavenumbers or latent variables employed in each model is indicated in parenthesis. *N* indicates the number of test samples employed in this study.

NIR DATA		LDA/SW (2)[a] Predicted class index			LDA/SPA (12) Predicted class index			LDA/GA (17) Predicted class index			PLS-DA (9) Predicted class index		
True class index	*N*	1	2	3	1	2	3	1	2	3	1	2	3
1	15	**14**	1	–	**15**	–	–	**15**	–	–	**15**	–	–
2	15	5	**10**	–	1	**14**	–	–	**15**	–	–	**15**	–
3	15	1	–	**14**	–	–	**15**	–	–	**15**	–	–	**15**

MIR DATA		LDA/SW (6)[b] Predicted class index			LDA/SPA (7) Predicted class index			LDA/GA (8) Predicted class index			PLS-DA (11) Predicted class index		
True class index	*N*	1	2	3	1	2	3	1	2	3	1	2	3
1	15	**15**	–	–	**15**	–	–	**15**	–	–	**15**	–	–
2	16	–	**16**	–	–	**16**	–	–	**16**	–	–	**16**	–
3	14	–	–	**14**	–	–	**14**	–	–	**14**	–	–	**14**

[a] The threshold value selected was 0.10.
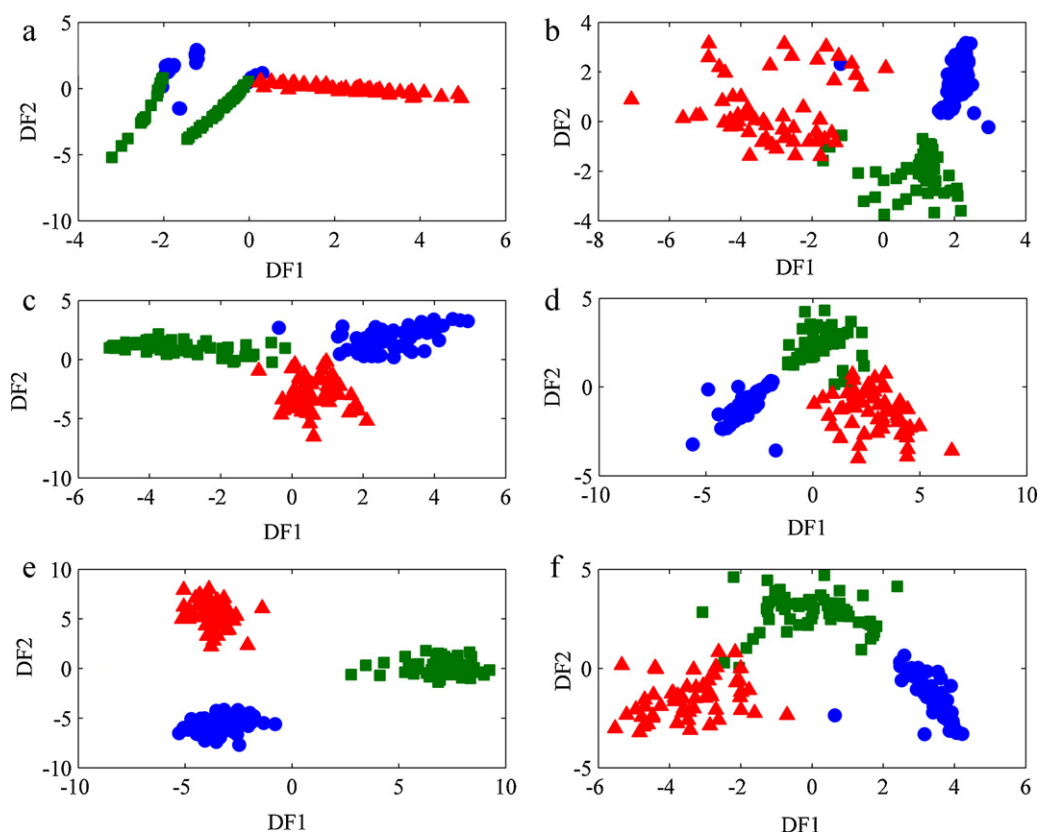[b] The threshold value selected was 0.90.

Fig. 4. DF2 × DF1 score plots for the overall data set in the region of NIR (a, c and e) and MIR (b, d and f) using wavenumbers selected by (a and b) SW; (c and d) SPA and (e and f) GA (● : authentic HEAF samples, ■ : HEAF samples adulterated with water, ▲ : HEAF samples contaminated with methanol).

data when LDA is applied to the variables selected by GA (Fig. 4e). In this case, the samples adulterated with water had been separated from the authentic samples and contaminated with methanol samples along DF1 direction. DF2 clearly distinguishes authentic samples from samples class adulterated with methanol.

4. Conclusions

This work presented a method based on multivariate classification methods (PLS-DA and LDA coupled with the variable selection algorithms) to detect adulteration in hydrated ethyl alcohol fuel samples employing NIR and MIR spectroscopies.

LDA/SW, LDA/SPA, LDA/GA, and PLS-DA models have achieved a correct prediction rate of 100% in the test set, when the MIR spectra were used. In case of the data set recorded using NIR region, correct prediction rates of 84.4% and 97.8% were achieved using LDA/SW and LDA/SPA models, respectively. PLS-DA and LDA/GA algorithms, however, correctly classified all samples in the test set.

The results obtained in this study indicate that the proposed method is a promising alternative to identify adulteration in hydrated ethyl alcohol fuel samples with water or methanol. Moreover, the appropriate use of variables selected by SPA, GA or SW algorithms can provide useful information for the development of portable and low cost instruments, such as an NIR photometer

that can be built using light emitting diodes (LED) in wavenumbers selected by these algorithms.

Acknowledgments

References

[1] R.M. Balabin, R.Z. Syunyaev, S.A. Karpov, Fuel 86 (2007) 323–327.
[2] R.M. Balabin, R.Z. Safieva, E.I. Lomakina, Chemom. Intell. Lab. Syst. 93 (2008) 58–62.
[3] I.C. Macedo, J.E.A. Seabra, J.E.A.R. Silva, Biomass Bioenergy 32 (2008) 582–595.
[4] Brazilian National Agency for Petroleum, Natural Gas and Biofuels (ANP). Available from: www.anp.gov.br (accessed 12.11.11).
[5] Brazilian National Agency for Petroleum, Natural Gas and Biofuels (ANP), Resolution No. 7 de 09.02.2011. Available from: www.anp.gov.br (accessed 22.11.11).
[6] N.P. Cheremisinoff, Industrial Solvents Handbook, 2nd ed., Marcel Dekker, New York, 2003.
[7] R.E. Gosselin, H.C. Hodge, R.P. Smith, M.N. Gleason, Clinical Toxicology of Commercial Products, Williams & Wilkins, Baltimore, 1976.
[8] ABNT NBR 5992, Álcool etílico e suas misturas com água – Determinação da massa específica e do teor alcoólico – Método do densímetro de vidro, 2007.
[9] R.M. Balabin, R.Z. Safieva, Energy Fuels 25 (2011) 2373–2382.
[10] R.M. Balabin, S.V. Smirnov, Anal. Chim. Acta 692 (2011) 63–72.
[11] P. Felizardo, P. Baptista, J.C. Menezes, M.J.N. Correia, Anal. Chim. Acta 595 (2007) 107–113.
[12] H.L. Fernandes, I.M. Raimundo Jr., C. Pasquini, J.J.R. Rohwedder, Talanta 75 (2008) 804–810.
[13] L.S. Mendes, F.C.C. Oliveira, P.A.Z. Suarez, J.C. Rubim, Anal. Chim. Acta 493 (2003) 219–231.
[14] H.S.P. Carneiro, A.R.B. Medeiros, F.C.C. Oliveira, G.H.M. Aguir, J.C. Rubim, P.A.Z. Suarez, Energy Fuels 22 (2008) 2767–2770.
[15] R.M. Balabin, E.I. Lomakina, Analyst 136 (2011) 1703–1712.
[16] R.M. Balabin, E.I. Lomakina, R.Z. Safieva, Fuel 90 (2011) 2007–2015.
[17] R.S. da Costa, S.R.B. Santos, L.F. Almeida, E.C.L. Nascimento, M.J.C. Pontes, R.A.C. Lima, S.S. Simões, M.C.U. Araújo, Microchem. J. 78 (2004) 27–33.
[18] R.G. Brereton, Chemometrics for Pattern Recognition, John Wiley & Sons Ltd., Bristol, UK, 2009.
[19] R.A. Fisher, Ann. Eugenics. 7 (1936) 179–188.
[20] M.-T. Sánchez, D.P. Marín, K.F. Rojas, J.-E. Guerrero, A.G. Varo, Talanta 78 (2009) 530–536.
[21] O. Galtier, O. Abbas, Y.L. Dréau, C. Rebufa, J. Kister, J. Artaud, N. Dupuy, Vib. Spectrosc. 55 (2011) 132–140.
[22] M.C. Ortiz, L. Sarabia, R. García-Rey, M.D.L. Castro, Anal. Chim. Acta 558 (2006) 125–131.
[23] P. Williams, P. Geladi, G. Fox, M. Manley, Anal. Chim. Acta 653 (2009) 121–130.
[24] M.C.U. Araújo, T.C.B. Saldanha, R.K.H. Galvão, T. Yoneyama, H.C. Chame, V. Visani, Chemom. Intell. Lab. Syst. 57 (2001) 65–73.
[25] R.K.H. Galvão, M.C.U. Araújo, in: S.D. Brown, R. Tauler, B. Walczak (Eds.), Comprehensive Chemometrics: Chemical and Biochemical Data Analysis, Elsevier, Oxford, 2009, pp. 233–283.
[26] M.J.C. Pontes, R.K.H. Galvão, M.C.U. Araújo, P.N.T. Moreira, O.D. Pessoa Neto, G.E. José, T.C.B. Saldanha, Chemom. Intell. Lab. Syst. 78 (2005) 11–18.
[27] M.S. Di Nezio, M.F. Pistonesi, W.D. Fragoso, M.J.C. Pontes, H.C. Goicoechea, M.C.U. Araujo, B.S. Fernández Band, Microchem. J. 85 (2007) 194–200.
[28] M.F. Pistonesi, M.S. Di Nezio, M.E. Centurión, A.G. Lista, W.D. Fragoso, M.J.C. Pontes, M.C.U. Araujo, B.S. Fernández Band, Talanta 83 (2010) 320–323.
[29] A.F.C. Pereira, M.J.C. Pontes, F.F.G. Neto, S.R.B. Santos, R.K.H. Galvão, M.C.U. Araújo, Food Res. Int. 41 (2008) 341–348.
[30] M.J.C. Pontes, A.M.J. Rocha, M.F. Pimentel, C.F. Pereira, Microchem. J. 98 (2011) 254–259.
[31] F.F. Gambarra-Neto, G. Marino, M.C.U. Araújo, R.K.H. Galvão, M.J.C. Pontes, E.P. Medeiros, R.S. Lima, Talanta 77 (2009) 1660–1666.
[32] M.J.C. Pontes, J. Cortez, R.K.H. Galvão, C. Pasquini, M.C.U. Araújo, R.M. Coelho, M.K. Chiba, M.F. Abreu, B.E. Madari, Anal. Chim. Acta 642 (2009) 12–18.
[33] E.D. Moreira, M.J.C. Pontes, R.K.H. Galvão, M.C.U. Araújo, Talanta 79 (2009) 1260–1264.
[34] U.T.C.P. Souto, M.J.C. Pontes, E.C. Silva, R.K.H. Galvão, M.C.U. Araújo, F.A.C. Sanches, F.A.S. Cunha, M.S.R. Oliveira, Food Chem. 119 (2010) 368–371.
[35] M.J.C. Pontes, C.F. Pereira, M.F. Pimentel, F.V.C. Vasconcelos, A.G.B. Silva, Talanta 85 (2011) 2159–2165.
[36] A.R. Caneca, M.F. Pimentel, R.K.H. Galvão, C.E. Matta, F.R. Carvalho, I.M. Raimundo Jr., C. Pasquini, J.J.R. Rohwedder, Talanta 70 (2006) 344–352.
[37] A. Savitzky, M.J.E. Golay, Anal. Chem. 36 (1964) 1627–1639.
[38] R.W. Kennard, L.A. Stone, Technometrics 11 (1969) 137–148.
[39] L.F.B. de Lira, F.V.C. Vasconcelos, C.F. Pereira, A.P.S. Paim, L. Stragevitch, M.F. Pimentel, Fuel 89 (2010) 405–409.
[40] Z. Xiaobo, Z. Jiewen, M.J.W. Povey, M. Holmes, M. Hanpin, Anal. Chim. Acta 667 (2010) 14–32.
[41] J. Workman, L. Weyer, Practical Guide to Interpretative Near-infrared Spectroscopy, CRC Press, New York, 2008.
[42] L.F.B. de Lira, M.S. de Albuquerque, J.G.A. Pacheco, T.M. Fonseca, E.H.S. Cavalcanti, L. Stragevitch, M.F. Pimentel, Microchem. J. 96 (2010) 126–131.